Making Every Event Count: Balancing Data Efficiency and Accuracy in Event Camera Subsampling

Supplementary Material

1. Details of Subsampling Parameters

Table 1 presents the specific parameters used for each subsampling method across various subsampling levels. The parameters are chosen to ensure that the average number of events $\langle N \rangle$ remains similar across different subsampling methods at each subsampling level for each dataset.

2. Memory Usage and Computational Complexity

In Table 2 of the main paper, we compare the memory usage and computational complexity across six different subsampling methods. We report the total memory units required for an event camera of size $H \times W$, and computational complexity in terms of multiply-accumulate operations (MACs) for a video with N number of events. Spatial, temporal, and random subsampling require only $\mathcal{O}(1)$ memory for storing a few method-specific parameters and essentially no specific MAC operation. Event Count method uses memory proportional to the downscaled spatial grid size $(\frac{H}{r_y}) \times (\frac{W}{r_x})$, and need N MAC operation for computing the normalized event count per each incoming event. The corner-based subsampling method adapted from [1] requires $\mathcal{O}(HW)$ memory for the event representation frame. The MAC number contains vertical and horizontal Sobel filtering $2\,\texttt{ksize}^2\,{w_c}^2\,N$, appyling filtering for computing the structural tensor $3\,\texttt{blockSize}^2\,{w_c}^2\,N$, and $10\,{w_c}^2\,N$ for other computations including Harris score calculation. The causal density-based subsampling also requires $\mathcal{O}(HW)$ memory for the method explained in Subsection 3.2 of the main paper. The computational complexity is $4\,{w_d}^2\,N$ MAC operations.

For an exemplary comparison between the computational operations of the corner-based and causal density-based methods, based on the chosen parameters in Table 1, the per-event computing cost for the corner-based method is $40\,{w_c}^2$, while for the causal density-based method, it is $4\,{w_d}^2$, where $w_c = w_d = 7$.

It is important to note that in Subsection 3.2 of the main paper, our focus was not on optimizing memory usage or computational complexity but rather on analyzing the accuracy performance of density-based methods across different subsampling levels. There are existing approaches aimed at developing efficient spatiotemporal filtering methods [2–4] that can improve both memory efficiency and computational complexity. For instance, in [3], the authors proposed a spatiotemporal filtering technique that reduces memory usage from $\mathcal{O}(HW)$ to $\mathcal{O}((HW)^{\frac{1}{2}})$.

3. Visualization of subsampling methods

Figure 1 provides a visualization of the effect of different subsampling methods on event data. In the first row, we show the original event data without any subsampling. Starting from the second row, the figure illustrates the results for two different subsampling levels applied to each dataset. Each image is labeled with the corresponding number of subsampled events, which are consistent across the different subsampling methods.

References

[1] Arren Glover, Aiko Dinale, Leandro De Souza Rosa, Simeon Bamford, and Chiara Bartolozzi. luvHarris: A Practical Corner Detector for Event-Cameras. *IEEE Transactions on Pattern Analysis and Machine Intelligence*, 44(12):10087–10098, 2022. Conference Name: IEEE Transactions on Pattern Analysis and Machine Intelligence. 1

[2] Shasha Guo and Tobi Delbruck. Low Cost and Latency Event Camera Background Activity Denoising. *IEEE Transactions on Pattern Analysis and Machine Intelligence*, 45(1):785–795, 2023. Conference Name: IEEE Transactions on Pattern Analysis and Machine Intelligence. 1

[3] Alireza Khodamoradi and Ryan Kastner. O(N)O(N)-Space Spatiotemporal Filter for Reducing Noise in Neuromorphic Vision Sensors. *IEEE Transactions on Emerging Topics in Computing*, 9(1):15–23, 2021. Conference Name: IEEE Transactions on Emerging Topics in Computing. 1

[4] Hongjie Liu, Christian Brandli, Chenghan Li, Shih-Chii Liu, and Tobi Delbruck. Design of a spatiotemporal correlation filter for event-based sensors. In *2015 IEEE International Symposium on Circuits and Systems (ISCAS)*, pages 722–725, 2015. 1

Table 1. Parameters of different subsampling methods for various subsampling levels: from 1 (most #events) to 6 (least #events). **mS**: milliseconds.

Subsampling methods	parameters	dataset	subsampling levels (1: most #events, 6: least #events)					
			1	2	3	4	5	6
Spatial	(r_x,r_y)	same for all	(2,2)	(4,3)	(6,6)	(12,10)	(15,12)	(25,16)
Temporal	r_t	same for all	4	12	36	120	180	400
	w_t (mS)	same for all	10	10	10	10	10	10
Random	ρ	same for all	$\frac{1}{4}$	$\frac{1}{12}$	$\frac{1}{36}$	$\frac{1}{120}$	$\frac{1}{180}$	$\frac{1}{400}$
Event Count	(r_x,r_y)	same for all	(2,2)	(4,3)	(6,6)	(12,10)	(15,12)	(25,16)
	$p_{EC}^{(\text{thresh})}$	same for all	0.75	0.75	1.0	1.0	1.0	1.0
Corner-based	w_c	same for all	7×7	7×7	7×7	7×7	7×7	7×7
	`ksize`	same for all	3	3	3	3	3	3
	`blockSize`	same for all	2	2	2	2	2	2
	`k`	same for all	0.04	0.04	0.04	0.04	0.04	0.04
	$h_c^{(\text{thresh})}$	N-Caltech101	0.067	0.23	0.68	1.52	3.85	9.10
		N-Cars	0.091	0.25	0.56	1.0	1.67	2.5
		DVS-Gesture	0.077	0.17	0.5	16.7	3.33	7.70
Causal density-based	τ (mS)	same for all	30	30	30	30	30	30
	w_d	same for all	7×7	7×7	7×7	7×7	7×7	7×7
	$f^{(\text{thresh})}$	N-Caltech101 & N-Cars	3.33	10.0	30.0	66.67	166.67	400.0
		DVS-Gesture	4.63	11.63	38.56	111.11	250.0	555.56

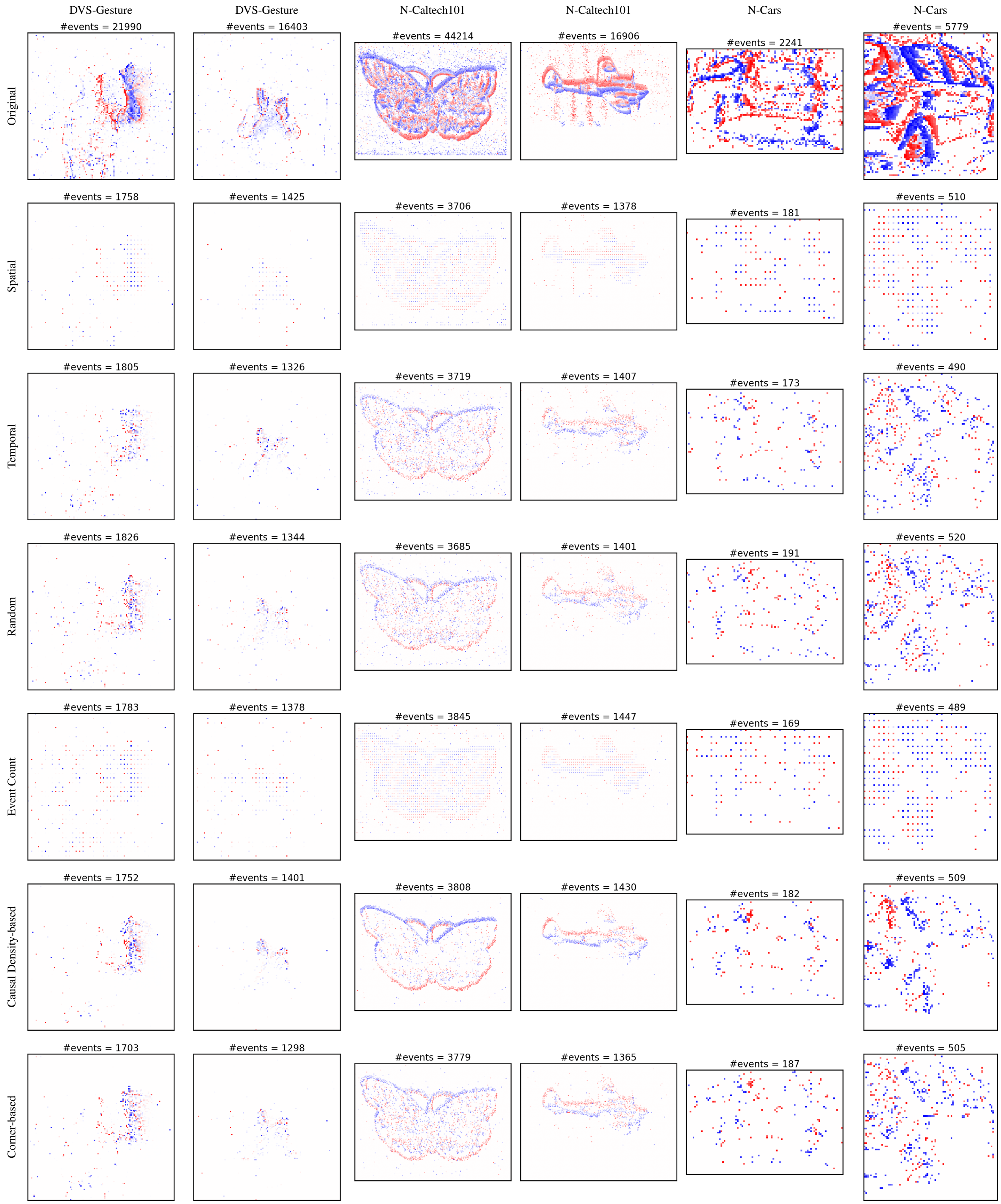

Figure 1. Visualization of different subsampling methods (starting from the second row). The first row shows the original data. We show for two videos for each dataset. The title of each image is the number of subsampled events. The number of events for different subsampling methods are similar.